Carnegie Mellon University
Research Showcase @ CMU

Computer Science Department | School of Computer Science

3-2007

Robust Estimation of Dominant Axis of Rotation

Lillian Y. Chang
Carnegie Mellon University

Nancy S. Pollard
Carnegie Mellon University, nsp@cs.cmu.edu

Follow this and additional works at: http://repository.cmu.edu/compsci

Published In
.

This Article is brought to you for free and open access by the School of Computer Science at Research Showcase @ CMU. It has been accepted for inclusion in Computer Science Department by an authorized administrator of Research Showcase @ CMU. For more information, please contact research-showcase@andrew.cmu.edu.

Robust estimation of dominant axis of rotation [1]

Lillian Y. Chang *, Nancy S. Pollard

School of Computer Science, Carnegie Mellon University, Pittsburgh, PA 15213

Abstract

A simple method is developed for robustly estimating a fixed dominant axis of rotation (AoR) of anatomical joints from surface marker data. Previous approaches which assume a model of circular marker trajectories use plane-fitting to estimate the direction of the AoR. However, when there is limited joint range of motion and rotation due to a second degree of freedom, minimizing only the planar error can give poor estimates of the AoR direction. Optimizing a cost function which includes the error component within a plane, instead of only the component orthogonal to a plane, leads to improved estimates of the AoR direction for joints which exhibit additional rotational motion from a second degree of freedom. Results from synthetic data validation show the ranges of motion where the new method has lower estimation error compared to plane-fitting techniques. Estimates of the flexion-extension AoR from empirical motion capture data of the knee and index finger joints were also more anatomically plausible.

Key words: Axis of rotation, Joint models, Optimization

1. Introduction

Many techniques for human movement analysis require a kinematic skeletal model for defining how the motion is measured. Parameters describing the joint locations and rotational axes can be adjusted to fit the subject's anthropomorphic dimensions. Subject-specific models can capture subtleties of an individual's motion that may not be preserved by using a generic skeleton.

Certain joints, such as the knee or finger joints, may be modeled with a single axis of rotation (AoR) that describes a fixed average location and orientation of an idealized hinge joint. This simplified model has been previously proposed for biomedical assessment by others (e.g., Schwartz and Rozumalski, 2005; Halvorsen, 2003; Gamage and Lasenby, 2002; Zhang et al., 2003), and the developed techniques are based on a single degree-of-freedom joint model. However, even though the movement is dominated by flexion-extension motion, these anatomic joints often exhibit more than one degree of freedom, such as rotation due to adduction-abduction. During a calibration session where the subject is asked to exercise the full joint range of motion, there will be movement about the dominant AoR and any secondary axes of rotation. In

* Corresponding author. Robotics Institute, Carnegie Mellon University, 5000 Forbes Avenue Pittsburgh, PA 15213.
Email address: lillianc@ri.cmu.edu (Lillian Y. Chang).

[1] Author personal corrected copy. Please see the Journal of Biomechanics homepage (http://www.sciencedirect.com/science/journal/00219290) for the authoritative version of the article (http://dx.doi.org/10.1016/j.jbiomech.2007.01.010).

these cases it is desirable to be able to estimate the dominant AoR robustly from movement which includes non-trivial motion in a secondary direction.

In this work we concentrate on functional methods for estimating a fixed average AoR of a joint. Functional methods fit models based on the relative motion between adjacent body segments and do not require surface marker alignment with respect to anatomic landmarks, as compared to predictive methods for finding subject-specific joint axes (e.g., Kadaba et al., 1990; Davis et al., 1991; Vaughan et al., 1999). In addition, functional methods are flexible for use with different anatomic joints and accommodate an arbitrary marker protocol.

A number of previous studies have also addressed average AoR estimation using functional methods. In one class of approaches, Halvorsen et al. (1999) and Schwartz and Rozumalski (2005) estimate the AoR as the line which best describes the collection of instantaneous rotational axes between pairs of frames. The approaches either require a choice of frame separation or usage of all possible pairs of frames, which can be computationally expensive. Another group of approaches determines joint coordinate systems using multiple optimization steps that solve for a high-dimensional set of variables and may include estimation of the joint angles at every frame in addition to the fixed joint parameters (e.g., Sommer and Miller, 1980; van den Bogert et al., 1994; Reinbolt et al., 2005). The AoR is a specified axis of the resulting joint coordinate system.

The approaches used by Gamage and Lasenby (2002) and Cerveri et al. (2005) both first estimate a point on the AoR by sphere-fitting and then find the AoR direction by plane-fitting, where the marker motion along the axis direction is minimized. O'Brien et al. (2000) propose a method for computing the AoR as a degenerate case of estimating a fixed joint center. The method was validated for synthetic data but was not successfully applied to empirical motion capture data due to significant motion along a second degree of freedom (O'Brien et al., 2000).

The new approach described in this paper is similar to that of Gamage and Lasenby (2002) and Cerveri et al. (2005) in that a point on the AoR is selected using sphere-fitting techniques developed for estimating the center of rotation (CoR). The key insight and focus of this work is the approach for estimation of the AoR direction given a point on AoR. Instead of only modeling the error along the AoR direction as in plane fitting, the circle-fitting approach also includes the error orthogonal to the AoR direction in the optimized cost function. The model is more appropriate for practical motion capture situations while still allowing a simple and intuitive implementation. Compared to plane-fitting (Gamage and Lasenby, 2002), circle-fitting estimates AoR directions reliably even when joints exhibit non-trivial rotation not described by the dominant AoR.

2. Method

2.1. *Cost function model*

Our model assumes that a marker attached to a moving body segment will travel around an AoR fixed in the reference body segment frame (Fig. 1). The AoR is a line defined by a point on the axis $\mathbf{m}$ and the unit direction of the axis $\mathbf{n}$. For an ideal hinge joint, each marker trajectory is a circular path on a plane orthogonal to the AoR. Multiple marker trajectories will be constrained to circles on parallel planes which each have normal $\mathbf{n}$, and the AoR passes through all of the circle centers. In practical situations, marker positions measured around an anatomic joint may deviate from their respective circles due to joint laxity or rotation in a secondary direction. The position $\mathbf{v}_k^p$ of the pth marker at frame k is offset from the circle by some error vector $\mathbf{e}_k^p$.

The AoR is estimated by finding the best-fitting circle to the marker trajectory. The trajectory around the AoR should have minimal distance from the plane of the circle as well as minimal deviation from the nominal radius r_p. Accordingly, we consider two components of each error vector $\mathbf{e}_k^p$. The planar error δ_k^p is the magnitude of $\mathbf{e}_k^p$ parallel to the AoR, and the radial error ε_k^p is the magnitude of $\mathbf{e}_k^p$ in the plane orthogonal to the AoR (Fig. 1).

If the two components of planar error and radial error are considered individually, the cost function

minimization would model either the best-fitting planes or the best-fitting cylinders, respectively, instead of the best-fitting circles. Such models might be adequate in situations where the joint has a large range of motion (RoM) but may become problematic when there is limited joint RoM (Fig. 2). Instead, we consider a more comprehensive cost function which describes how well a set of P marker trajectories over N time frames fits a set of circles:

$$f = \sum_{p=1}^{P} \sum_{k=1}^{N} \left((\delta_k^p)^2 + (\varepsilon_k^p)^2 \right). \tag{1}$$

This combined cost function models how well the marker trajectories each maintain a fixed distance from the AoR and also remain on a plane orthogonal to the AoR. The contribution of an individual data point $\mathbf{v}_k^p$ to the cost function is equivalent to the squared length of the error vector $\mathbf{e}_k^p$.

2.2. *Planar cost formulation*

The planar error for a given marker trajectory describes the total deviation of the marker positions from the best-fitting plane. Given the direction of the plane normal $\mathbf{n}$, the deviation can be calculated as the difference between the component of $\mathbf{v}_k^p$ parallel to $\mathbf{n}$ and some nominal distance of the plane from origin, μ_p (Fig. 3). The total of squared planar errors over all trajectories is

$$f_p = \sum_{p=1}^{P} \sum_{k=1}^{N} (\delta_k^p)^2 = \sum_{p=1}^{P} \sum_{k=1}^{N} (\mathbf{v}_k^p \cdot \mathbf{n} - \mu_p)^2. \tag{2}$$

The best-fitting plane minimizes the cost f_p. The optimal value of μ_p can be found from setting the derivative of (2) with respect to μ_p equal to zero:

$$\mu_p = \left(\frac{1}{N} \sum_{k=1}^{N} \mathbf{v}_k^p \right) \cdot \mathbf{n} = \overline{\mathbf{v}^p} \cdot \mathbf{n}. \tag{3}$$

The optimal value of μ_p is the component of the marker trajectory centroid $\overline{\mathbf{v}^p}$ parallel to $\mathbf{n}$. Each trajectory can be expressed relative to its respective centroid (Fig. 3):

$$\mathbf{u}_k^p = \mathbf{v}_k^p - \overline{\mathbf{v}^p}. \tag{4}$$

Then the planar cost function can be computed for a given AoR direction candidate $\mathbf{n}$ by:

$$f_p = \sum_{p=1}^{P} \sum_{k=1}^{N} (\delta_k^p)^2 = \sum_{p=1}^{P} \sum_{k=1}^{N} (\mathbf{u}_k^p \cdot \mathbf{n})^2. \tag{5}$$

This is mathematically equivalent to the cost function used by Gamage and Lasenby (2002) for finding the AoR direction. The total planar error given by (5) can be rewritten in matrix form using a standard formulation from fitting of algebraic surfaces (see, e.g., Pratt, 1987). Let D_p denote the data matrix whose rows contain the pth marker's positions relative to the trajectory centroid:

$$D_p = \begin{bmatrix} (\mathbf{u}_1^p)^{\mathrm{T}} \\ \vdots \\ (\mathbf{u}_k^p)^{\mathrm{T}} \\ \vdots \\ (\mathbf{u}_N^p)^{\mathrm{T}} \end{bmatrix}, \tag{6}$$

such that the PN planar errors are given by

$$D\mathbf{n} = \begin{bmatrix} D_1 \\ \vdots \\ D_p \\ \vdots \\ D_P \end{bmatrix} \mathbf{n}. \tag{7}$$

Then the total planar cost in (5) is equivalent to

$$f_p = \|D\mathbf{n}\|^2 = \mathbf{n}^{\mathrm{T}} D^{\mathrm{T}} D\mathbf{n} = \mathbf{n}^{\mathrm{T}} S\mathbf{n} \tag{8}$$

where S is the matrix $D^{\mathrm{T}}D$.

For a given data set, the matrix S is constant and can be precomputed before the iterative optimization. This allows the planar cost function to be evaluated quickly for any candidate direction $\mathbf{n}$ by a simple inner product $\mathbf{n}^{\mathrm{T}} S\mathbf{n}$.

2.3. *Radial cost formulation*

The radial error measures how much the distance from the marker trajectory to the AoR varies relative to the best-fitting cylinder whose axis of symmetry is the AoR. Given the direction of the axis $\mathbf{n}$ and any point on the line $\mathbf{m}$, the shortest vector from a single marker position to the line is given by

$$\mathbf{w}_k^p = (I - \mathbf{n}\mathbf{n}^{\mathrm{T}})(\mathbf{v}_k^p - \mathbf{m}) \tag{9}$$

where I is the 3×3 identity matrix. The matrix $I - \mathbf{n}\mathbf{n}^{\mathrm{T}}$ operates on a vector by subtracting the component of the vector parallel to direction $\mathbf{n}$ so that the result is the component of the vector orthogonal to $\mathbf{n}$. The total of squared radial errors for a set of marker trajectories is then

$$f_r = \sum_{p=1}^{P}\sum_{k=1}^{N} (\varepsilon_k^p)^2 = \sum_{p=1}^{P}\sum_{k=1}^{N} \left(\|(I - \mathbf{n}\mathbf{n}^{\mathrm{T}})(\mathbf{v}_k^p - \mathbf{m})\| - r_p\right)^2. \tag{10}$$

The optimal radius r_p can be calculated for each trajectory by setting the derivative of (10) with respect to r_p equal to zero:

$$r_p = \frac{1}{N}\sum_{k=1}^{N} \|(I - \mathbf{n}\mathbf{n}^{\mathrm{T}})(\mathbf{v}_k^p - \mathbf{m})\|. \tag{11}$$

2.4. *Calculation of a point on the AoR*

The combined cost function is the sum of (2) and (10) such that both the planar error along the AoR direction and the radial error orthogonal to the AoR direction are considered:

$$\begin{aligned} f &= \sum_{p=1}^{P}\sum_{k=1}^{N} (\delta_k^p)^2 + (\varepsilon_k^p)^2 \\ &= \mathbf{n}^{\mathrm{T}} S\mathbf{n} + \sum_{p=1}^{P}\sum_{k=1}^{N} \left(\|(I - \mathbf{n}\mathbf{n}^{\mathrm{T}})(\mathbf{v}_k^p - \mathbf{m})\| - r_p\right)^2. \end{aligned} \tag{12}$$

Since the ideal circular marker paths maintain constant distances from any single point on the AoR, $\mathbf{m}$ can be estimated using existing sphere-fitting methods for estimating the center of rotation (CoR) (e.g., Chang and Pollard, in press; Halvorsen, 2003; Gamage and Lasenby, 2002; Cerveri et al., 2005). In our implementation, we use the method by Chang and Pollard (in press) because of its robustness to different joint ranges of motion.

3. Validation and results

The proposed method is tested on both simulated data sets and empirical motion capture data. The method was implemented using MATLAB 6.5 (Mathworks, Inc.; Natick, MA) and uses the MATLAB *fminsearch* function for the iterative optimization. Our implementation uses 10 different initializations for the optimization in order to avoid local minima and increase the quality of the solution. The 10 initial

directions for **n** were defined by the 10 pairs of vertices of a regular dodecahedron centered at the origin. These give a consistent set of evenly-distributed directions that is simple to compute.

The results of minimizing the combined cost function in (12) are compared to the AoRs estimated from minimizing only the planar error (as in Gamage and Lasenby, 2002) and minimizing only the radial error. The methods are compared on multiple data sets to illustrate the respective ranges of applicability.

3.1. *Simulation tests*

Synthetic data sets simulated marker trajectories for joints which may be modeled as having a dominant AoR with additional secondary rotation. The nominal surface marker positions are based on marker protocols for the knee joint and the index finger metacarpo-phalangeal (MCP) joint. The simulated knee model assumes the AoR is fixed with respect to the upper leg reference frame such that surface markers on the lower leg follow circular paths (Fig. 4a). For the index MCP joint model, the AoR is fixed in the hand dorsum frame and the simulated trajectories model the movement of markers on the proximal phalanx (Fig. 4b). For both the knee and index MCP joints, the flexion-extension (FE) axis is considered the dominant AoR while adduction-abduction (AA) rotation has a smaller RoM.

Each synthetic data set simulated joint rotation with FE RoM of 30°, 60°, or 90°, and AA RoM with ratio of 0.1, 0.3, 0.5, or 0.7 relative to the FE RoM. For each error condition of an FE RoM paired with a relative AA RoM ratio, 30 independent error sequences were added to the nominal rotated marker positions. The directions of the error vectors were uniformly distributed and the error magnitudes were normally distributed with standard deviation of 1.0 mm. Each data set had 121 frames.

Performance of the AoR estimation methods is measured by the angular offset between the estimated axis direction and the nominal axis direction used to generate the synthetic data set. This angular AoR error is computed for each data set, and the 30 AoR errors are averaged for a given error condition.

The results (Fig. 5, Table 1) show that the AoR error for all three methods increases for larger relative AA RoM ratio. This is expected as the increasing motion due to the secondary direction makes the model of circular marker paths less applicable. Most notably, there is often a quick transition between error conditions for which the AoR error is less than 20° to conditions where the the error is greater than 50°. The key difference between using the planar cost only and using the combined cost is the point at which such a transition occurs. Minimizing only the planar cost results in less than 5° AoR error only for the test conditions with 0.1 ratio of AA RoM to FE RoM. However, optimizing the combined cost function of planar error and radial error results in an average AoR error of less than 5° for up to 0.3 RoM ratio in all three tested FE RoM cases and additionally, less than 10° for 0.5 RoM ratio for the 30° and 60° absolute FE RoM cases.

In addition, minimizing only the radial cost resulted in average AoR error greater than that from using the combined cost function for the two lowest RoM ratios. For the synthetic data sets, the proposed method extends the robustness of the circle-fitting model to a larger range of secondary adduction-abduction rotation. The difference in the average AoR error between the synthetic knee data and the synthetic index MCP data was less than 1.5° for all test conditions.

3.2. *Empirical joint axis estimation*

Measured motion of the knee and index finger was used for additional validation. The first experiment tested the estimation of the flexion-extension axis of the knee for an able-bodied male subject. Reflective markers were attached to the subject's right leg (Fig. 4a). The subject was directed to exercise the full active RoM of the right leg, without specific attention to a particular joint or direction of motion. The empirical evaluation uses only the marker motion of the lower leg in the frame of the upper leg.

In a second set of experiments, the flexion-extension axes of the index finger were estimated for three male and three female able-bodied subjects. Small reflective markers were attached to the right hand (Fig.

4b). Each subject was asked to exercise the full active RoM of the entire index finger at a self-selected speed and without directed concentration on a single joint or rotational direction. The AoR was estimated for all three index finger joints from the marker trajectories of the distal body segment in the frame of the proximal body segment.

Axes estimated by the proposed method were overall more consistently plausible than the AoRs resulting from minimizing either the planar cost only or the radial cost only (Figs. 6 and 7). For the empirical knee motion, the secondary adduction-abduction was large enough that the axis normal to best-fitting plane unintuitively passes through the marker paths instead of maintaining a constant distance from them (Fig. 6). In contrast, incorporating the radial error into the minimized cost function more accurately models the circular-path model such that the marker trajectories maintain approximately-fixed distances from the AoR.

Results from the index finger motion show how the applicability of the plane-fitting method changes with different joint RoM conditions, while the new method provides more anatomically-plausible estimates of the finger flexion-extension axes (Fig. 7). The results for each of the three tested methods were consistent across the multiple subjects tested (Fig. 8). The direction of estimated axes are represented by projection angles with respect to a coordinate frame defined by markers on the hand dorsum and with the finger in an extended position (Figs. 7 and 8). Note that for this choice of coordinate frame, we expect ϕ to be near 90° and θ to be near 0°. However, the angles estimated from the method minimizing planar cost are more scattered and do not always reflect these expected values, especially for the index finger MCP joint. Depending on the joint, minimizing only the planar cost or only the radial cost can result in reasonable AoR estimates. However, consideration of the combined cost function improves the consistency of the results with respect to multiple joints.

The empirical data sets had between 1000 to 5000 frames of data, and the computational time for the proposed method ranged from 4 to 25 seconds.

4. Discussion

The model of circular marker trajectories can be used for robust AoR estimation when both the planar error along the AoR direction and the radial error orthogonal to AoR direction are incorporated in the cost function. Many joints modeled as single hinge joints have large RoMs for the dominant AoR yet the amount of secondary rotation is sufficiently large to compromise the accuracy of techniques that only consider the planar error. Including the radial error in the cost function increases the accuracy and robustness of the AoR estimate for a wider range of plausible motion capture situations. The iterative optimization does require additional computation compared to the plane-fitting method, which has a direct solution. However, the proposed method preserves the intuition of circle-fitting, is simple to implement, and the additional computational cost is small.

Computation of the radial error does depend on a reliable estimate of the CoR as a point on the AoR. In our tested situations, the sphere-fitting solution by Chang and Pollard (in press) provided an adequate CoR location to use in the optimization without refinement. The estimate of a point on the AoR could be included as a variable within the optimization procedure for further refinement, when the increased dimensionality of the iterative search is acceptable.

This study has focused on methods for fitting a fixed model which describes the average position and orientation of a joint's axis of rotation. This model is appropriate for applications where the joint angles are used to describe the subject's movement with respect to a fixed skeletal model for a given individual. Our method could be used to fit subject-specific joint models for applications such as character animation for

computer graphics and haptic interfaces. For example, for a full hand model which includes the motion of all finger segments, a simple low-dimensional model for each joint is desirable and intuitive for the system user to control. Furthermore, fitting a fixed dominant axis joint model using the new method may provide an alternative to other techniques proposed for clinical assessment (e.g., Gamage and Lasenby, 2002; Halvorsen, 2003; Zhang et al., 2003), and further validation studies are recommended.

The applicability of the new method is limited to cases where the secondary RoM is less than 50% of the dominant RoM, based on the simulation tests. Motion with conditions outside this range involve more complex geometric constraints on the shape of the marker trajectories. Estimating the dominant AoR for rotations with fully two degrees of freedom may require models beyond the simple circle-fitting approach, such as the higher dimensional optimizations proposed by Sommer and Miller (1980), van den Bogert et al. (1994), and Reinbolt et al. (2005). In addition, the assumption of an average AoR may not be appropriate for applications where the migration of the joint axis significantly impacts the accuracy of the model. Since the proposed method only estimates a fixed dominant AoR, an alternative approach for these cases is the estimation of the instantaneous screw axis between pairs of time frames to describe the varying parameters of a full six degree-of-freedom joint model (e.g. Woltring et al., 1985; Teu and Kim, 2006).

We note that the proposed method was tested on a limited set of marker protocols. The simplicity and flexibility of functional methods such as circle-fitting depend on the assumption that surface marker positions can be used to determine a coordinate frame for a rigid body segment. The performance of such methods may be significantly affected by the selected marker protocol due to soft tissue artifacts. The empirical results on two anatomic joints and multiple subjects suggest the proposed method's potential. Further investigation is required to thoroughly evaluate its performance in the presence of systematic error due to skin motion. Other factors such as the geometric properties of the marker cluster relative to the joint location (Camomilla et al., 2006) should also be considered. Additionally, extensions of this work may focus on validation of the method for estimating the dominant axis for pathological joints.

Acknowledgements

This work was supported by the National Science Foundation (CCF-0343161, IIS-0326322, ECS-0325383, and CNS-0423546). L.Y. Chang is supported by a National Science Foundation Graduate Research Fellowship. The authors would like to thank Moshe Mahler for creating the subject models and Alias / Wavefront for donating the Maya software.

References

Camomilla, V., Cereatti, A., Vannozzi, G., Cappozzo, A., 2006. An optimized protocol for hip joint centre determination using the functional method. Journal of Biomechanics (39), 1096–1106.

Cerveri, P., Lopomo, N., Pedotti, A., Ferrigno, G., 2005. Derivation of centers and axes of rotation for wrist and fingers in a hand kinematic model: Methods and reliability results. Annals of Biomedical Engineering 33 (3), 402–412.

Chang, L. Y., Pollard, N. S., in press. Constrained least-squares optimization for robust estimation of center of rotation. Journal of Biomechanics. doi:10.1016/j.jbiomech.2006.05.010

Davis, R. B., Ounpuu, S., Tyburski, D., Gage, J. R., 1991. A gait analysis data collection and reduction technique. Human Movement Science 10 (5), 575–587.

Gamage, S. S., Lasenby, J., 2002. New least squares solutions for estimating the average centre of rotation and the axis of rotation. Journal of Biomechanics 35 (1), 87–93.

Halvorsen, K., 2003. Bias compensated least squares estimate of the center of rotation. Journal of Biomechanics 36 (7), 999–1008.

Halvorsen, K., Lesser, M., Lundberg, A., 1999. A new method for estimating the axis of rotation and the center of rotation. Journal of Biomechanics 32 (11), 1221–1227.

Kadaba, M. P., Ramakrishnan, H. K., Wootten, M. E., 1990. Measurement of lower extremity kinematics during level walking. Journal of Orthopedic Research 8 (3), 383–392.

O'Brien, J. F., Bodenheimer, R. E., Brostow, G. J., Hodgins, J. K., 2000. Automatic joint parameter estimation from magnetic motion capture data. In: Proceedings of Graphics Interface 2000. Canadian Human-Computer Communications Society, Lawrence Erlbaum Associates, Montreal, Quebec, Canada, pp. 53–60.

Pratt, V., 1987. Direct least-squares fitting of algebraic surfaces. In: Computer Graphics (SIGGRAPH '87 Proceedings). Vol. 21. ACM, Addison Wesley, Anaheim, California, USA, pp. 145–152.

Reinbolt, J. A., Schutte, J. F., Fregly, B. J., Koh, B. I., Haftka, R. T., George, A. D., Mitchell, K. H., 2005. Determination of patient-specific multi-joint kinematic models through two-level optimization. Journal of Biomechanics 38 (3), 621–626.

Schwartz, M. H., Rozumalski, A., 2005. A new method for estimating joint parameters from motion data. Journal of Biomechanics 38 (1), 107–116.

Sommer, H. J., Miller, N. R., 1980. A technique for kinematic modeling of anatomical joints. Journal of Biomechanical Engineering 102 (4), 311–317.

Teu, K. K., Kim, W., 2006. Estimation of the axis of a screw motion from noisy data – A new method based on Plucker lines. Journal of Biomechanics 39 (15), 2857–2862.

van den Bogert, A. J., Smith, G. D., Nigg, B. M., 1994. In vivo determination of the anatomical axes of the ankle joint complex: an optimization approach. Journal of Biomechanics 27 (12), 1477–1488.

Vaughan, C. L., Davis, B. L., O'Connor, J. C., 1999. Dynamics of Human Gait, 2nd Edition. Kiboho Publishers, Cape Town, South Africa.

Woltring, H., Huiskes, R., de Lange, A., 1985. Finite centroid and helical axis estimation from noisy landmark measurements in the study of human joint kinematics. Journal of Biomechanics 18 (18), 379–389.

Zhang, X., Lee, S. W., Braido, P., August 2003. Determining finger segmental centers of rotation in flexion-extension based on surface marker measurement. Journal of Biomechanics 36 (8), 1097–1102.

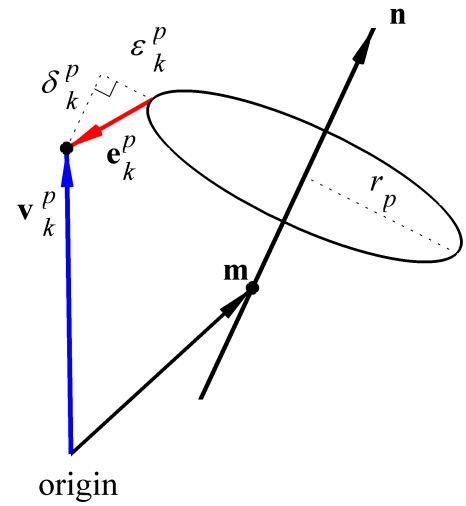

Fig. 1. Model of the pth marker at time k around an axial joint. The axis line is defined by point $\mathbf{m}$ and direction $\mathbf{n}$. The marker position $\mathbf{v}_k^p$ is constrained to a circle of radius r_p on a plane normal to $\mathbf{n}$, with some error vector $\mathbf{e}_k^p$. The two components of $\mathbf{e}_k^p$ are the planar error δ_k^p parallel to the AoR and the radial error ε_k^p orthogonal to the AoR.

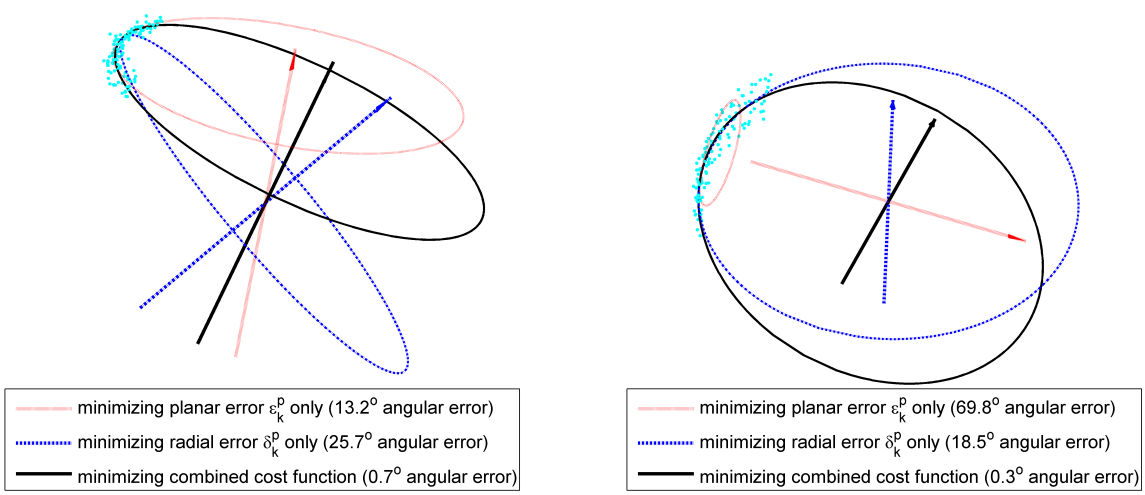

a b

Fig. 2. An example comparison of the best-fitting plane (minimizing planar error), best-fitting cylinder (minimizing radial error), and best-fitting circle (minimizing a combined cost function) for two sets of synthetic data with known AoR. The AoR direction estimated from the best-fitting circle method has the least angular error. In the second set (b), there is limited range of the dominant direction of motion combined with the additional motion due to a second rotational degree of freedom. For these conditions, minimizing planar error fits a circle in a plane which is nearly orthogonal to that containing the ideal circular arc.

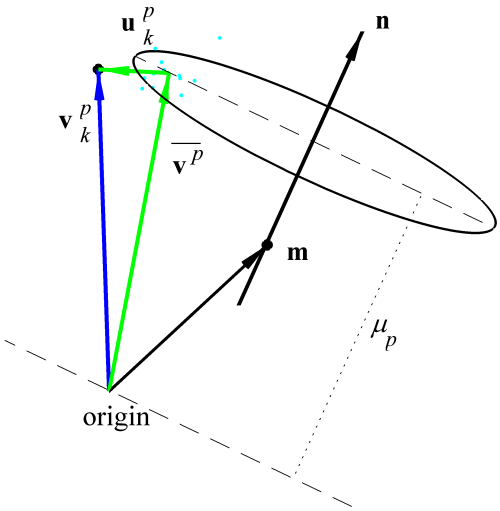

Fig. 3. Model of a plane with normal $\mathbf{n}$ and nominal distance from the origin μ_p. The data point $\mathbf{v}_k^p$ can be described in terms of the offset $\mathbf{u}_k^p$ from the data set centroid $\overline{\mathbf{v}^p}$.

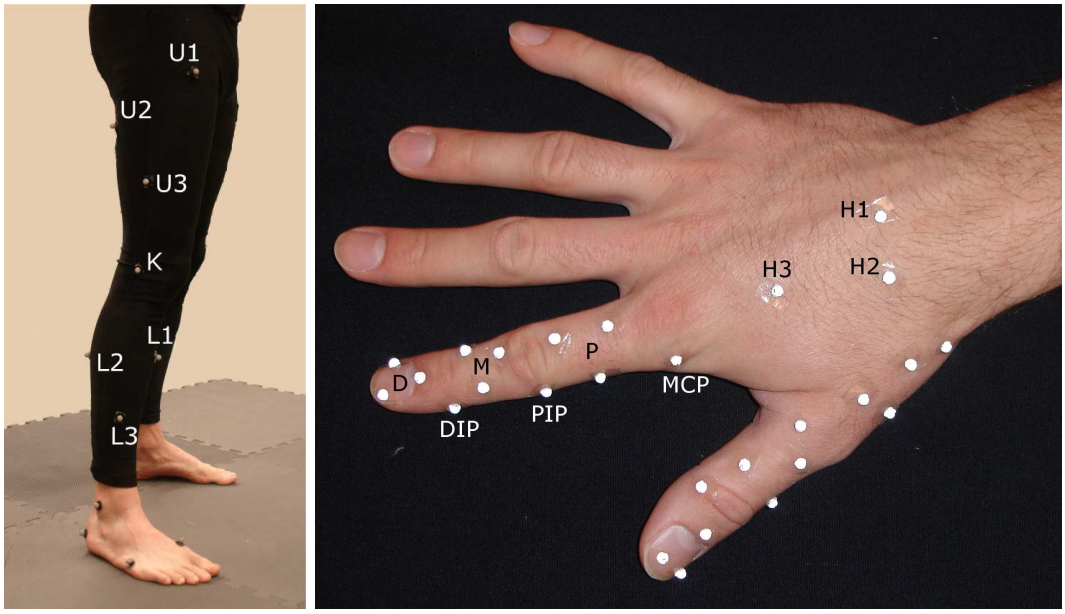

a b

Fig. 4. (a) Marker protocol for the knee joint. Markers U1, U2, and U3 define the frame for the upper leg, and markers L1, L2, and L3 are attached to the lower leg. The K marker is attached to the side of the knee. (b) Marker protocol for the index finger. Three surface markers are attached to each of four body segments: hand dorsum (H), proximal phalanx (P), middle phalanx (M), and distal phalanx (D) . In addition, single markers are attached at the metacarpal-phalangeal (MCP), proximal interphalangeal (PIP), and distal interphalangeal (DIP) joints.

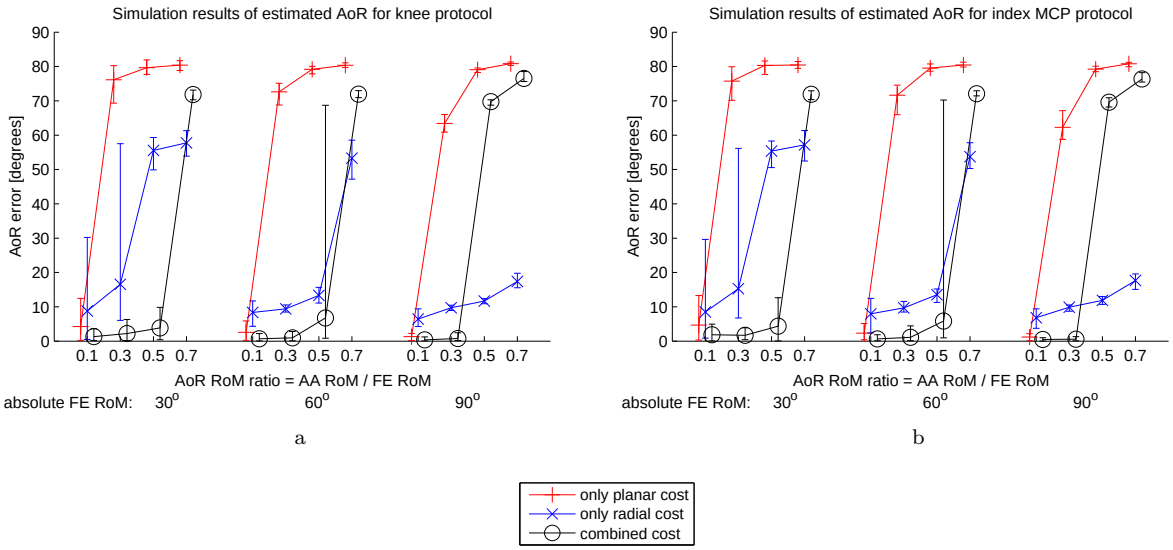

Fig. 5. Simulated data results for AoR estimation of flexion-extension axes for (a) the knee joint and (b) the index finger MCP joint. The trend lines show the average AoR angular error for the 30 trials in each error condition (Table 1). The error bars denote the minimum and maximum AoR angular error for each error condition.

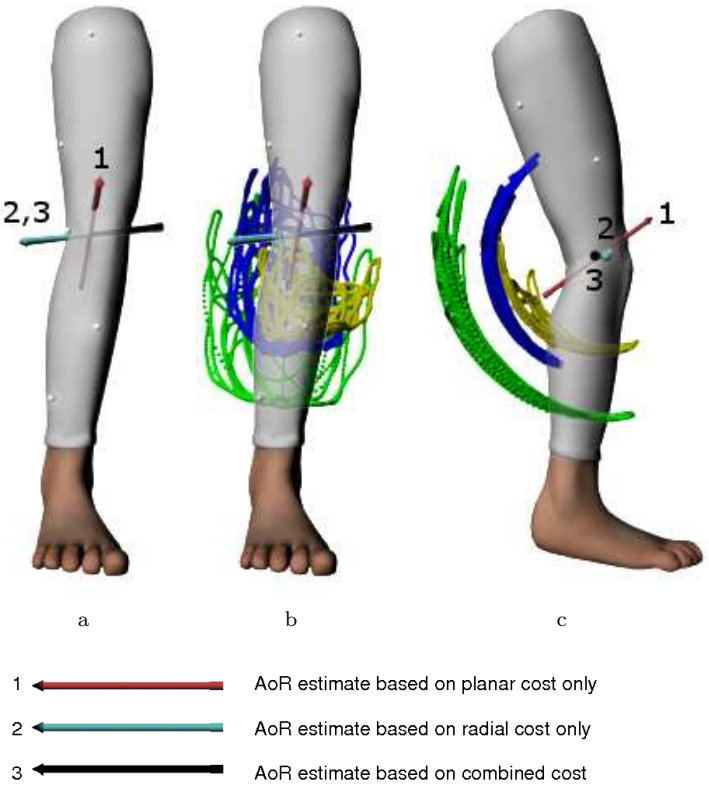

Fig. 6. Empirical results for AoR estimation of flexion-extension axes for the knee joint. Marker trajectories of the calf markers relative to the thigh frame exhibit both a dominant direction of flexion-extension motion as well as secondary adduction-abduction rotation. (a, b) Front view of the leg. (c) Side view of the leg. The AoR estimated from the combined cost optimization is nearly orthogonal with the plane of the page.

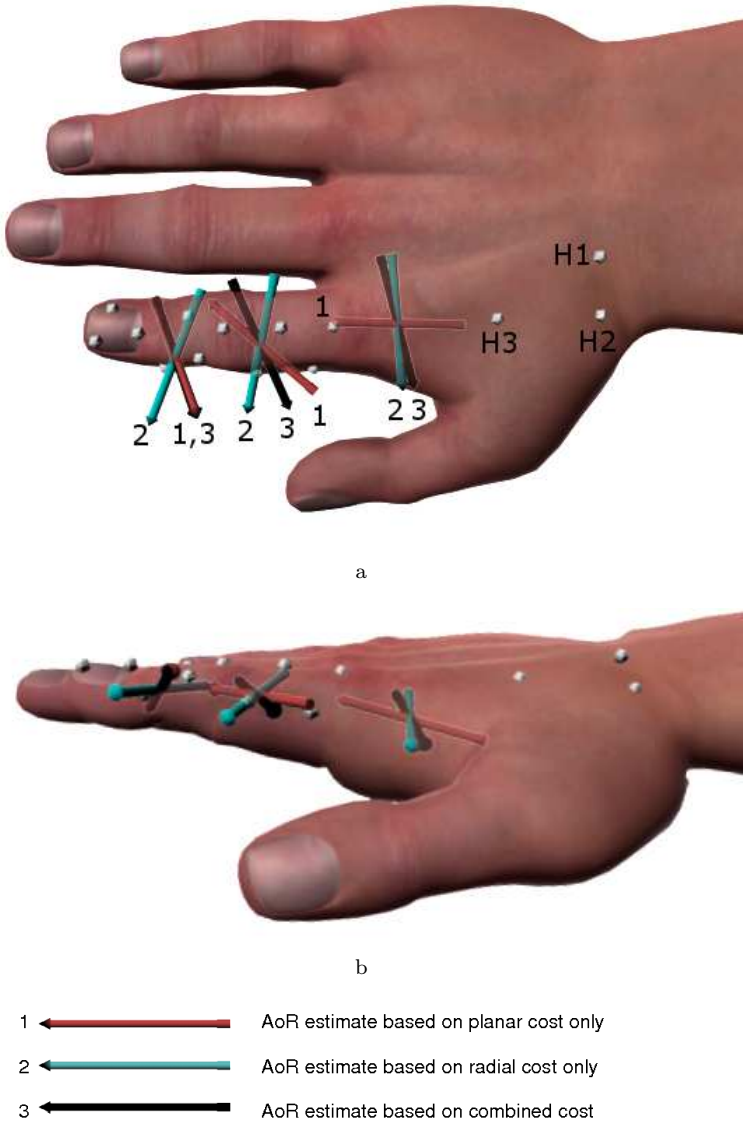

Fig. 7. Empirical results for AoR estimation of flexion-extension axes for the three index finger joints for an example subject. (a) Top view of the hand model. (b) Side view of the hand.

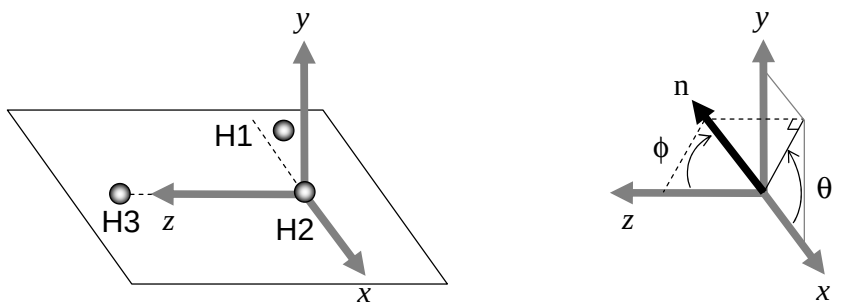

a

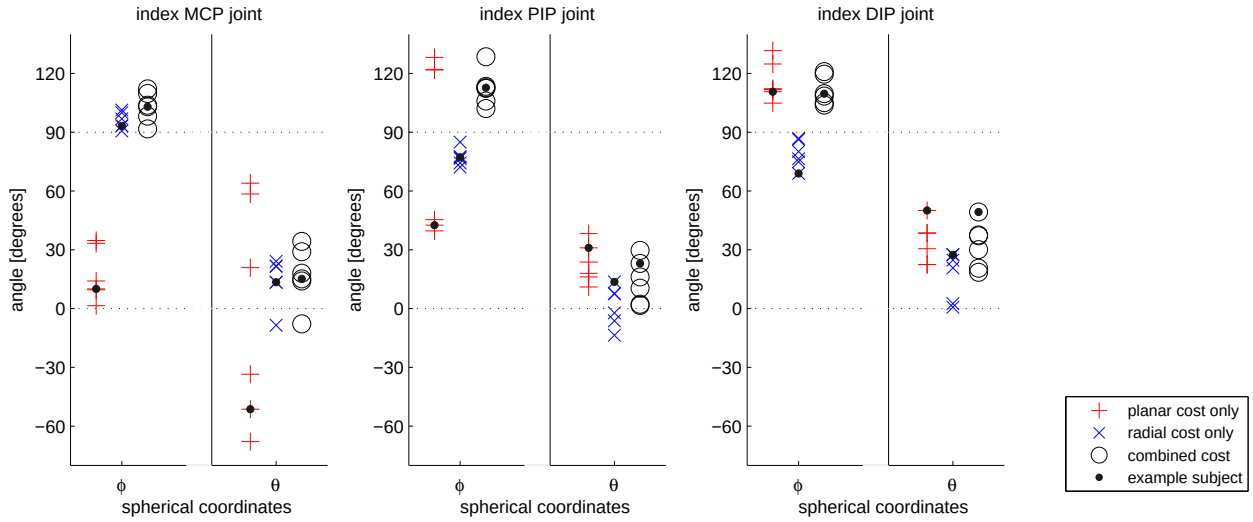

b

Fig. 8. Empirical results for AoR estimation of index finger joints. (a) Spherical angles ϕ and θ describe the direction of axis $\mathbf{n}$ with respect to a coordinate system defined by markers on the hand dorsum (Fig. 4b). The z axis is defined by markers $H3$ and $H2$, and the y axis is orthogonal to the plane of all three markers. The angle ϕ describes the orientation of an axis $\mathbf{n}$ with respect to the z axis, and θ denotes the angle between the projection of $\mathbf{n}$ onto the x-y plane and the x axis. (b) Comparison of AoR estimation results for index finger joints across six subjects, with the example subject (Fig. 7) highlighted. The spherical angles are measured for a reference pose where the finger is extended.

Table 1
Simulation test results of AoR estimation for the knee joint and index finger MCP joint using three optimization functions.

Optimization function	Mean and standard deviation of the AoR angular error for 30 trials in each error condition (degrees)											
	absolute FE RoM											
	30°				60°				90°			
	RoM ratio = AA RoM / FE RoM											
	.1	.3	.5	.7	.1	.3	.5	.7	.1	.3	.5	.7
knee protocol												
planar	4.3	76.1	79.7	80.4	2.6	72.6	79.2	80.3	1.3	63.4	79.1	80.8
	(3.4)	(2.6)	(0.9)	(0.7)	(1.2)	(1.5)	(0.4)	(0.3)	(0.5)	(1.3)	(0.4)	(0.2)
radial	8.8	16.6	55.5	57.7	8.4	9.4	13.3	53.3	6.4	9.7	11.7	17.4
	(6.9)	(18.2)	(1.9)	(2.1)	(2.1)	(0.6)	(1.1)	(2.5)	(1.3)	(0.4)	(0.4)	(0.9)
combined	1.3	2.2	3.8	71.8	0.7	1.0	6.7	72.0	0.4	0.8	69.8	76.5
	(1.0)	(1.5)	(2.6)	(0.7)	(0.5)	(0.7)	(12.1)	(0.4)	(0.3)	(0.5)	(0.4)	(0.7)
index MCP protocol												
planar	4.7	75.7	80.3	80.5	2.3	71.6	79.5	80.4	1.2	62.3	79.2	80.8
	(2.9)	(2.3)	(0.9)	(0.6)	(1.1)	(1.7)	(0.6)	(0.4)	(0.6)	(1.6)	(0.5)	(0.3)
radial	8.5	15.3	55.4	57.1	8.0	9.7	13.5	53.7	6.8	9.9	11.9	17.7
	(6.2)	(15.5)	(2.0)	(2.2)	(2.4)	(0.7)	(1.0)	(2.1)	(1.4)	(0.4)	(0.5)	(1.0)
combined	1.9	1.7	4.3	71.9	0.7	1.1	5.9	72.1	0.5	0.6	69.6	76.4
	(1.4)	(1.0)	(3.2)	(0.6)	(0.5)	(0.9)	(12.4)	(0.4)	(0.3)	(0.4)	(0.6)	(0.6)